Supplementary Information

Fixed-point "Blasting" Triggered by the Second Near-Infrared Light for Augmented Interventional Photothermal Therapy

Yongbin Cao,[†, #] Boshu Ouyang,[§,ǂ,#] Xiaowei Yang,[†] Qin Jiang,[†] Lin Yu,[†,] Shun Shen,[§,*] Jiandong Ding[†] and Wuli Yang[†,*]*

[†]State Key Laboratory of Molecular Engineering of Polymers & Department of Macromolecular Science, Fudan University, Shanghai 200433, PR China.

[§]The Institute for Translational Nanomedicine, Shanghai East Hospital, Tongji University School of Medicine, Shanghai, 200120, China.

[ǂ]Central Laboratory, First Affiliated Hospital, Institute (college) of Integrative Medicine, Dalian Medical University, Dalian, 116021, China. [#]Both authors contributed equally to this work.

*Corresponding Authors.

E-mail: yu_lin@fudan.edu.cn (L. Yu); sshen@tongji.edu.cn (S. Shen); wlyang@fudan.edu.cn (W. L. Yang)

Synthesis of PLGA-PEG-PLGA copolymer. The detailed procedure was described as the following: 25 g of PEG 1500 was added into a three-neck flask and heated at 130 °C for 3 h under vacuum to eliminate the remanent moisture. Then, LA (45.46 g) , GA (12.21 g) and catalytic amount of $Sn(Oct)_2$ were put into and maintained at 100 °C under vacuum for another 30 min. Next, the reaction system was stirred continuously and heated at 150 °C under the argon atmosphere for 12 h. After that, the reaction products were washed by 80 °C water for 4 times, and then lyophilized to obtain the final copolymer (PLGA-PEG-PLGA).

Characterization of PLGA-PEG-PLGA copolymer. ^{1}H-NMR spectra measured by a 400 MHz spectrometer (Bruker, AVANCE III) were used to investigate the chemical structure and composition of PLGA-PEG-PLGA copolymer. $CDCl_3$ and tetramethylsilane (TMS) were used as the solvent and the internal standard, respectively. The gel permeation chromatography system (GPC, Agilent1260) with a differential refractometer was used to determine the MW and distribution of the copolymer. The measurement was performed at 35 °C and tetrahydrofuran was used as the eluent at a flow rate of 1.0 mL/min. Monodispersed polystyrene was used as the standard for MW calculation. Rheological properties of the different composites were measured by a dynamic rheometer (Kinexus, Malvern) equipped with a Peltier cone-plate (angle: 1°, 60 mm diameter, 0.03 mm gap). Samples were loaded and sealed with a thin layer of silicone oil to prevent water evaporation. The measurements were carried out at an oscillatory frequency of 10 rad/s and a heating rate of 0.5 °C/min from 15 °C to 45 °C.

CLSM Imaging & Flow Cytometry Analysis. Prior to CLSM imaging or flow cytometry analysis, cells were cultured in 35-mm glass bottomed dishes at a density of 2×10^5 /dish for 24 h, and then randomly divided into five groups: laser group, Gel-AINP/FMCP group, Gel-FMCP + laser group, Gel-AINP + laser group and Gel-AINP/FMCP + laser group. Afterwards, cells were stained with Calcein-AM (10 mM in PBS) and PI (2 μM in PBS) for 15 min at 37 °C under 5% CO_2 atmosphere. For CLSM imaging, cells were subjected to imaging analysis with a confocal microscopy after replacing the staining solution with free RPMI-1640. Calcein-AM was excited by a 488 nm laser and the green emission (520 nm) was collected with a band pass-filter within the range 500-550 nm. PI was excited by a 564 nm laser and the red emission (620 nm) was collected with a band pass-filter within the range 600-700 nm. For flow cytometry analysis, after cells were stained with Annexin V-FITC/PI apoptosis detection kit, cells were directly digested and analyzed by a Gallios flow cytometry with excitation at 488 nm and emission at 525 ± 40 nm and 620 ± 30 nm, respectively. WinMDI software (version 2.9) was used to calculate cell apoptosis rate.

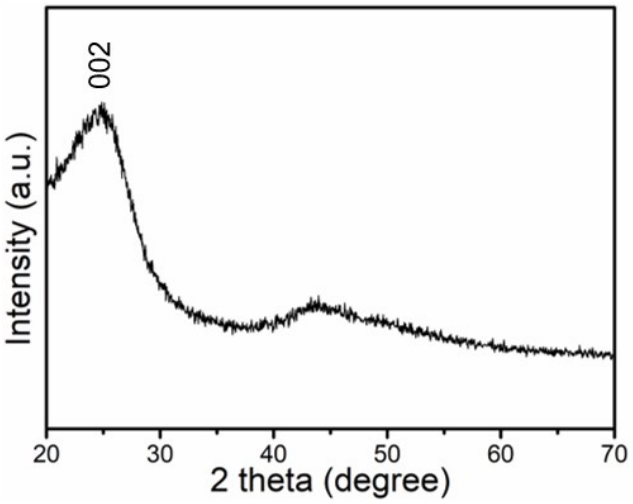

Fig. S1. XRD spectrum of AINP.

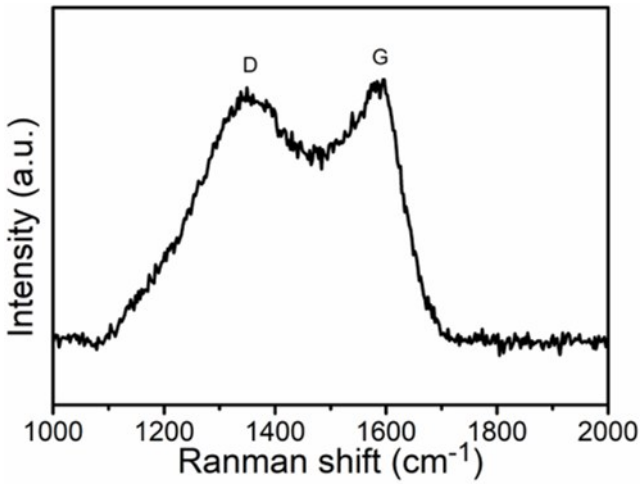

Fig. S2. Raman spectrum of AINP.

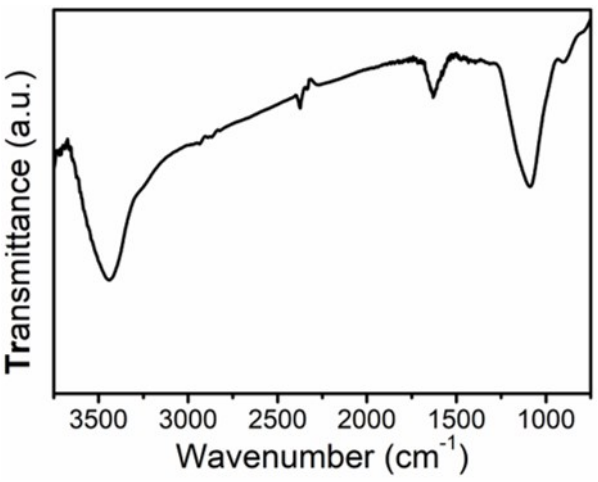

Fig. S3. FT-IR spectrum of AINP.

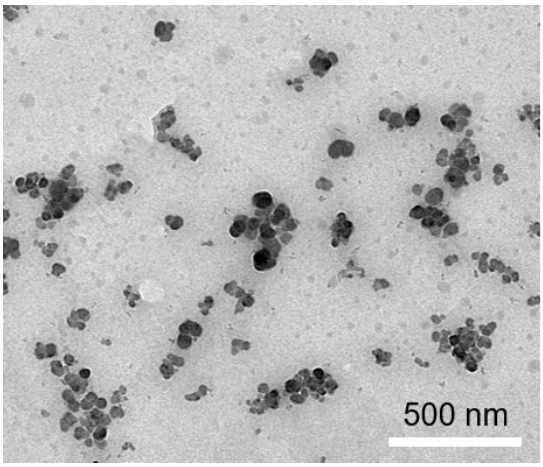

Fig. S4. TEM photograph of AINP.

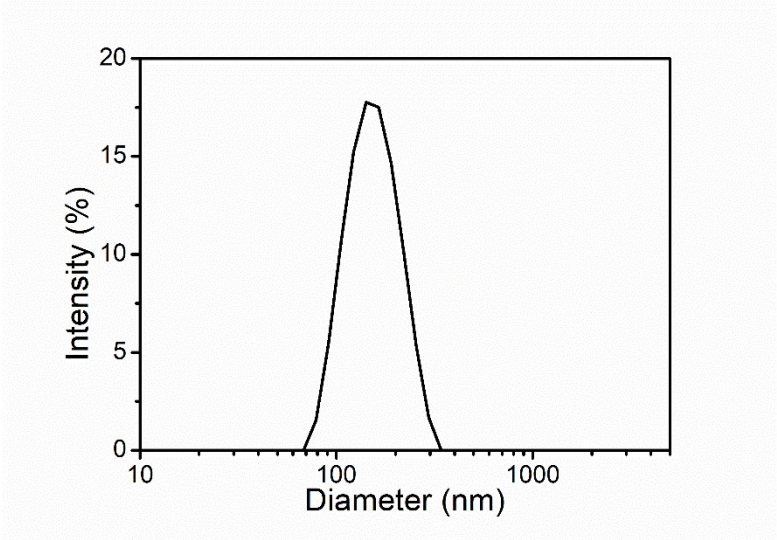

Fig. S5. Size distribution of AINP dispersion by DLS.

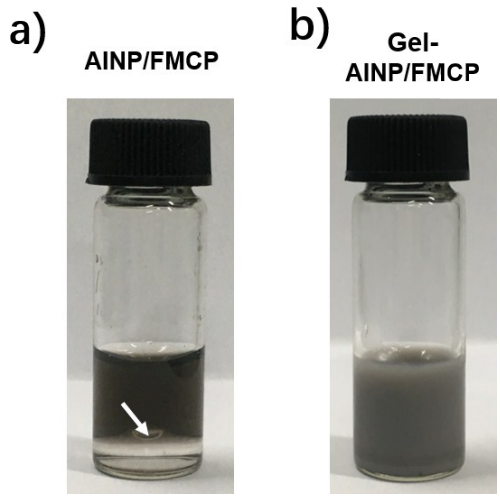

Fig. S6. Photographs of AINP/FMCP solutions with or without PLGA-PEG-PLGA copolymer.

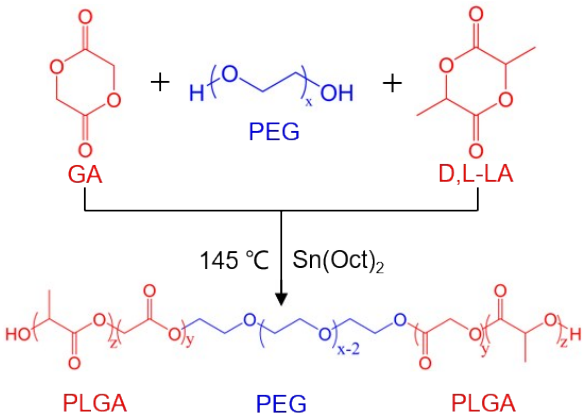

Fig. S7. Synthesis route of PLGA-PEG-PLGA copolymer.

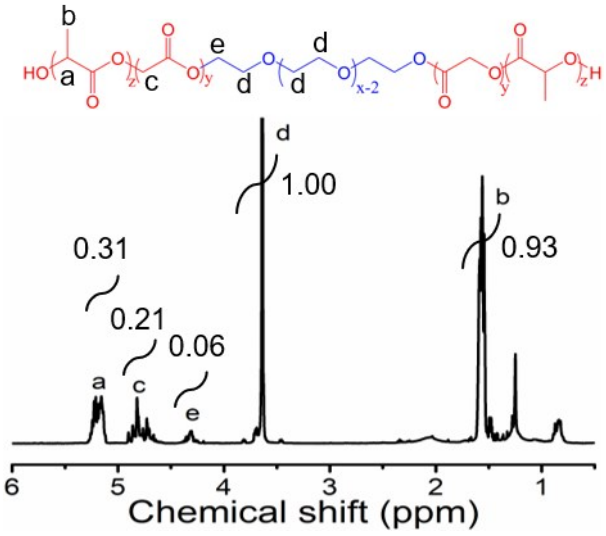

Fig. S8. ^{1}H NMR spectrum of PLGA-PEG-PLGA copolymer.

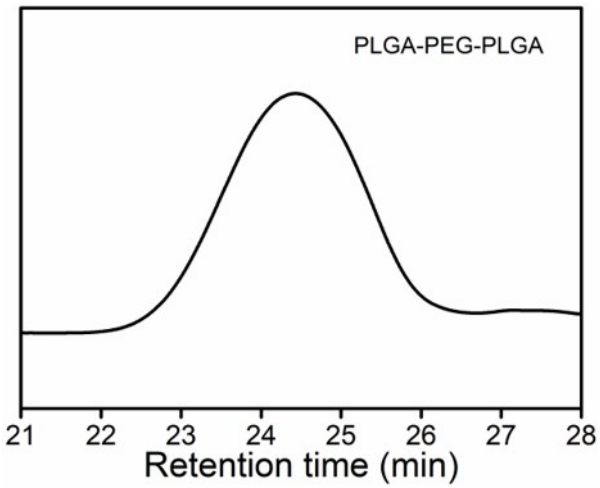

Fig. S9. GPC trace of PLGA-PEG-PLGA copolymer.

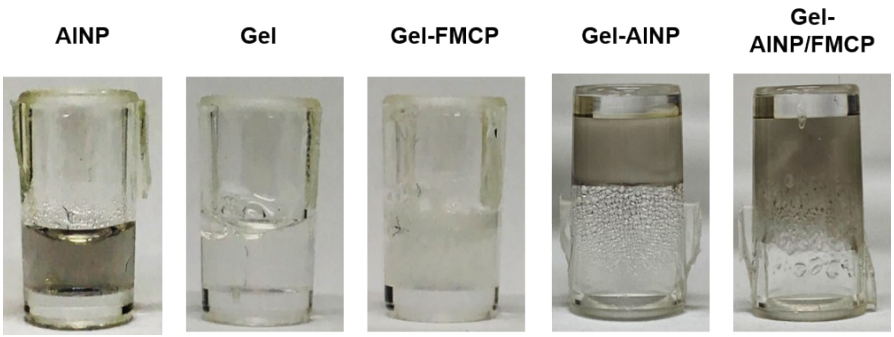

Fig. S10. Typical images of the sol and gel states of AINP solution and various copolymer solutions after exposure to NIR laser.

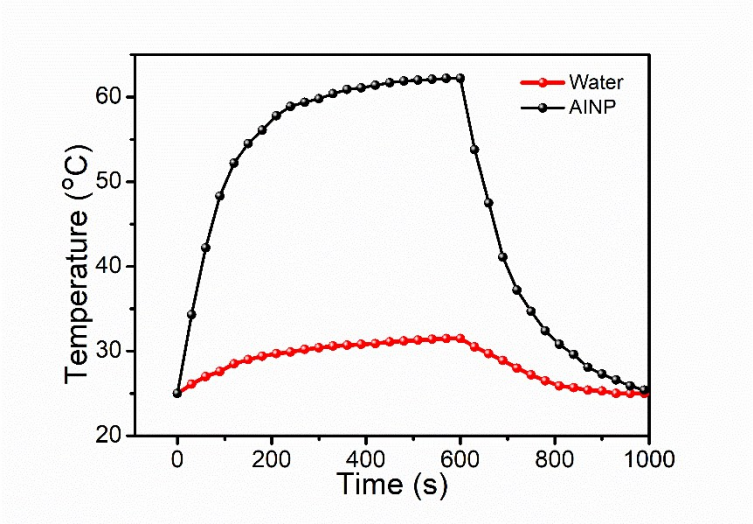

Fig. S11. Temperature elevation and decline curves of AINP dispersion exposed to a 1064 nm laser (50 μg/mL, 1 W/cm^2).

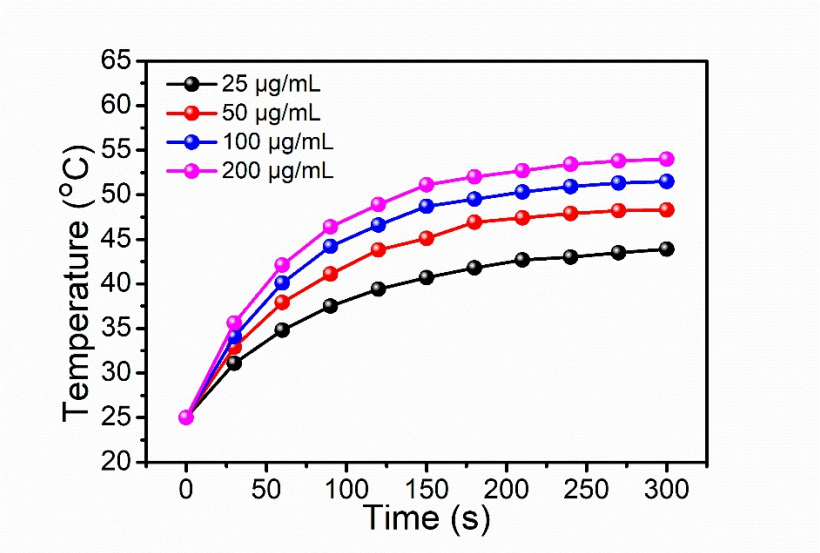

Fig. S12. Temperature change of hydrogel system containing various concentrations of AINP upon exposure to a 1064 nm laser (PLGA-PEG-PLGA: 25 wt%; FMCP: 5 v/v%; 0.5 W/cm^2).

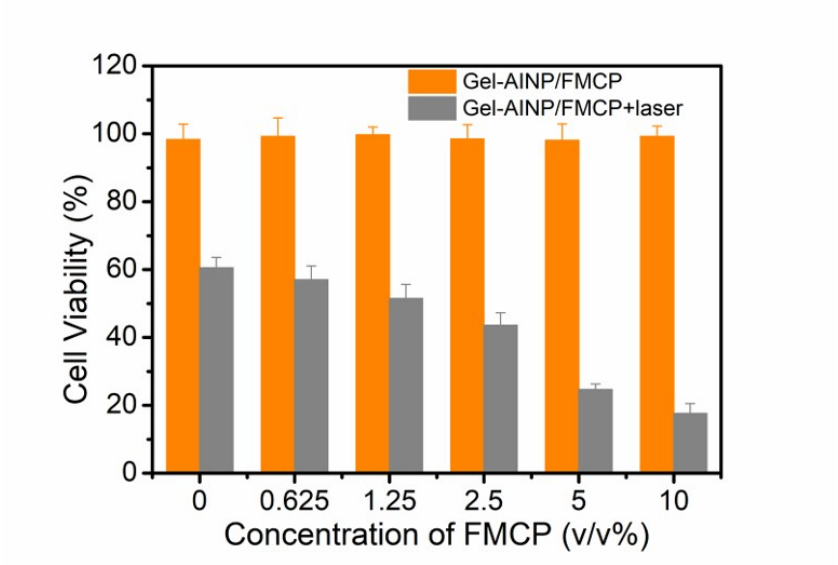

Fig. S13. The respective cell viability of HCT-116 cancer cells after treated with different concentrations of FMCP followed by a 1064 nm laser irradiation (0.5 W/cm^2; 5 min).

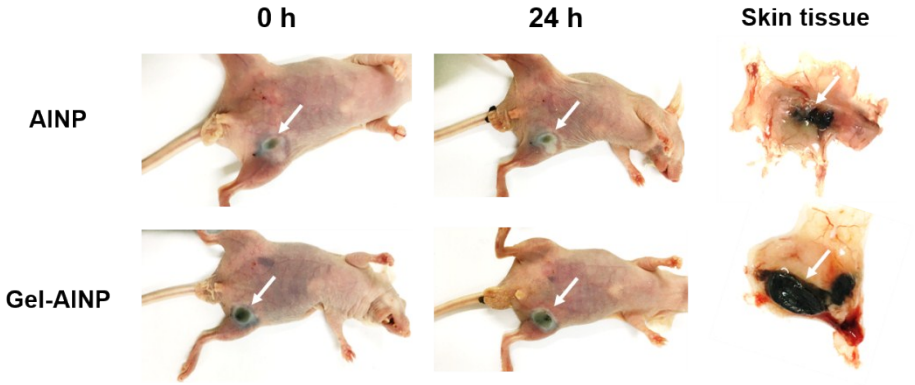

Fig. S14. Photographs of mice and their skin tissue after subcutaneously injected with AINP and Gel-AINP, and further exposed to NIR laser.

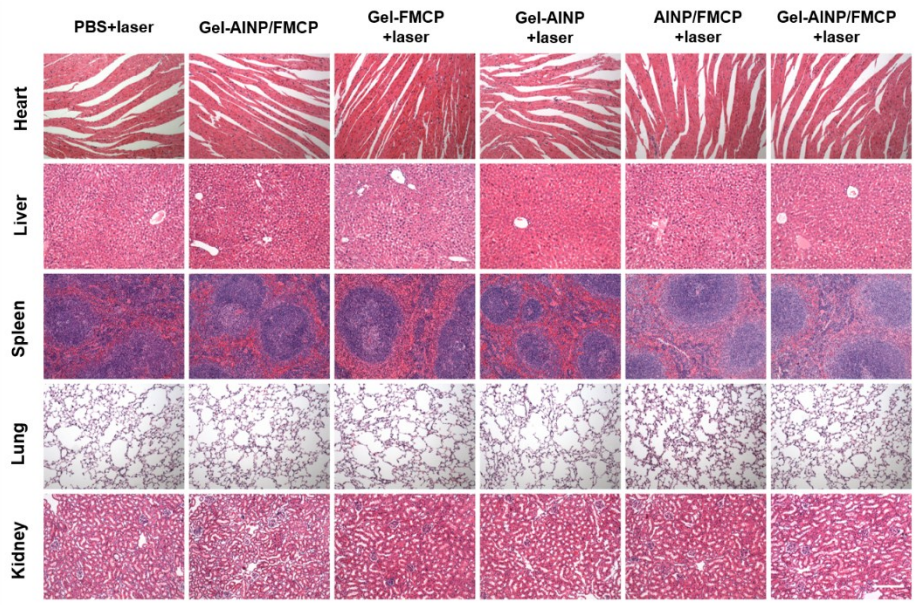

Fig. S15. H&E staining of the main organs of mice after different treatments. All the scale bars are 200 μm.

Table S1 Molecular parameters of PLGA-PEG-PLGA copolymer.

PEG M_n[a]	M_n[a]	LA/GA (mol/mol)[a]	M_n[b]	(M_w/M_n)[b]
1500	1830-1500-1830	2.98	4420	1.21

[a] Number-averaged molecular weight, M_n of the central block PEG was provided by Aldrich. Molar ratio of lactide/glycolide (LA/GA) and M_n of each PLGA block were calculated by ^{1}H NMR.

[b] Measured by GPC.

Table S2 Photothermal conversion efficiency of AINP and previous reported photothermal agents.

Photothermal agents	Laser wavelength (nm)	Photothermal conversion efficiency (η)	Reference
Fe_3O_4@CuS	1064	19.2 %	S1
IONP@shell-in-shell	1064	28.3 %	S2
Bi	1064	32.2 %	S3
SPN-OT	1064	36 %	S4
Au-Cu_9S_5	1064	37 %	S5
MoO_x	1064	37.4 %	S6
$(NH_4)_xWO_3$	1064	39.4 %	S7
Ti_3C_2@Au	1064	39.6 %	S8
Cu_3BiS_3	1064	40.7 %	S9
Nb_2C	1064	45.6 %	S10
SPN-DT	1064	49 %	S4
TBDOPV−DT	1064	50 %	S11
SPN-PT	1064	53 %	S4
PPy	1064	64.6 %	S12
AINP	1064	47.6 %	This work

References

S1 X. G. Ding, C. H. Liow, M. X. Zhang, R. J. Huang, C. Y. Li, H. Shen, M. Y. Liu, Y Zou,. N. Gao, Z. J. Zhang, Y. G. Li, Q. B. Wang, S. Z. Li and J. Jiang, *J. Am. Chem. Soc.*, 2014, **136**, 15684-15693.

S2 M. F. Tsai, C. Hsu, C. S. Yeh, Y. J. Hsiao, C. H. Su and L. F. Wang, *ACS Appl. Mater. Interfaces*, 2019, **10**, 1508-1519.

S3 X. J. Yu, A. Li, C. Z. Zhao, K. Yang, X. Y. Chen and W. W. Li, *ACS Nano*, 2017, **11**, 3990-4001.

S4 Y. Y. Jiang, P. K. Upputuri, C. Xie, Z. L. Zeng, A. Sharma, X. Zhen, J. C. Li, J. G. Huang, M. Pramanik, K. Y. Pu, *Adv. Mater.*, 2019, **31**, 1808166.

S5 X. G. Ding, C. H. Liow, M. X. Zhang, R. J. Huang, C. Y. Li, H. Shen, M. Y. Liu, Y. Zou, N. Gao, Z. J. Zhang, Y. G. Li, Q. B. Wang, S. Z. Li and J. Jiang, *J. Am. Chem. Soc.*, 2014, **136**, 15684-15693.

S6 J. E. Park, M. Kim, J. H. Hwang and J. M. Nam, *Small Methods*, 2017, **1**, 1600032.

S7 C. S. Guo, H. J. Yu, B. Feng, W. D. Gao, M. Yan, Z. W. Zhang, Y. P. Li, S. Q. Liu, *Biomaterials*, 2015, **52**, 407-416.

S8 W. T. Tang, Z. L. Dong, R. Zhang, X. Yi, K. Yang, M. L. Jin, C. Yuan, Z. D. Xiao, Z. Liu and L. Cheng, *ACS Nano*, 2019, **13**, 284-294.

S9 J. J. Zhou, Y. Y. Jiang, S. Hou, P. K. Upputuri, D. Wu, J. C. Li, P. Wang, X. Zhen, M. Pramanik, K. Y. Pu and H. W. Duan, *ACS Nano*, 2018, **12**, 2643-2651.

S10 H. Lin, S. S. Gao, C. Dai, Y. Chen and J. L. Shi, *J. Am. Chem. Soc*., 2017, **139**, 16235-16247.

S11 T. T. Sun, J. H. Dou, S. Liu, X. Wang, X. H. Zheng, Y. P. Wang, J. Pei and Z. G. Xie, *ACS Appl. Mater. Interfaces*, 2018, **10**, 7919-7926.

S12 X. Wang, Y. C. Ma, X. Sheng, Y. C. Wang, H. X. Xu, *Nano Lett.*, 2018, **18**, 2217-2225.